Thermal and dynamic mechanical properties of blends of bitumen with metallocene catalyzed polyolefins

Chiara Spadaro · Christopher J. G. Plummer ·
Jan-Anders E. Månson

Abstract A high penetration grade bitumen has been blended with up to 50 wt% of two different grades of metallocene catalyzed linear low density polyethylene (m-LLDPE) in order to investigate the potential of these and similar copolymers as a substitute for styrene butadiene styrene triblock copolymers in polymer-modified bitumens (PMB). A continuous polymer-rich phase was observed at m-LLDPE contents as low as 5–10 wt%, along with a significant decrease in the effective glass transition temperature of the PMBs with increasing polymer concentration, suggesting benefits for low temperature flexibility. The m-LLDPE-based PMBs also showed relatively low dynamic shear viscosities up to high polymer contents in the range of temperature and shear rate corresponding to typical PMB processing conditions. However, the presence of bitumen in the m-LLDPE-rich phase led to a significant reduction in the melting points of the m-LLDPE, and softening of the PMBs at temperatures as low as 40–50 °C, depending on the composition and the melting point of the pure polymer. PMBs based on the m-LLDPE with the higher melting point remained fully elastic in this temperature range, but at the expense of increased crystallinity and a higher glass transition temperature, which limit improvements in low temperature flexibility. On the other hand, the potentially broad composition and property windows associated with m-LLDPEs suggest considerable scope for the fine tuning of PMB properties by using combinations of different m-LLDPEs and/or other polyolefins as a means to optimize performance.

C. Spadaro · C. J. G. Plummer (✉) · J.-A. E. Månson
Laboratoire de Technologie des Composites et Polymères (LTC), École Polytechnique Fédérale de Lausanne (EPFL), Station 12, 1015 Lausanne, Switzerland
e-mail: christopher.plummer@epfl.ch

Introduction

Bitumen is a naturally occurring viscoelastic material whose chemical composition and structure are complex and variable, depending on the source of the crude oil from which it is derived, and on modifications induced by treatments in the refinery or during its service life [1]. The components of bitumen range from saturated hydrocarbons to polynuclear aromatics [2], and it is generally characterized on the basis of "SARA" fractionation in terms of what are termed (i) "saturates," "aromatics," and "resins," referred to collectively as "maltene," and (ii) "asphaltene," the fraction that is insoluble in *n*-heptane [3]. The corresponding microstructures are widely assumed to consist of a colloidal dispersion of micelles of asphaltene in a matrix that consists essentially of maltene, whose average molar mass is relatively low [1, 4, 5]. On the other hand, more recent studies indicate asphaltenes to be soluble in maltenes, so that the concept of a colloidal dispersion and the distinction between asphaltenes and maltenes solely in terms of polarity may be misleading [6, 7].

In applications such as road surfacing and roofing, bitumen is typically blended with polymers in order to improve properties such as flexibility at low temperature, *T*, and high *T* stiffness, while maintaining weldability and minimizing shrinkage. Polymer-modified bitumens (PMB) may also show improvements in thermal and fatigue cracking behavior, and increased resistance to high *T* aging [2, 3, 8–14]. The polymer most widely used in PMBs is styrene butadiene styrene (SBS) triblock copolymer, a thermoplastic elastomer in which the polystyrene end-blocks act as thermally reversible physical crosslinks and the rubbery polybutadiene mid-blocks provide the elasticity [1]. Although it does not fully dissolve, SBS swells to up to nine times its initial volume when blended with

Table 1 Physical properties of the polymer modifiers

	Comonomers	T_g (°C)	T_m (°C)	MFI (g/10 min)
PE–O	Ethylene–octene	−36	96	30
PE–B	Ethylene–butene	−53	35	5

bitumen, so that even at relatively low SBS concentrations (usually 5–6 wt%), the swollen polymer may form a continuous phase, significantly modifying the overall properties [2, 5]. Unsaturated elastomers such as SBS are nevertheless susceptible to environmental degradation, particularly under mechanical stress, and are relatively expensive. There is consequently interest in blending bitumen with other polymers, and, in particular, polyolefins, which are available in large quantities at relatively low cost, and show a wide range of mechanical properties depending on the details of their structure [8, 10, 15–27]. However, polyolefins are widely reported to show poor dispersions in bitumen, and PMBs based on such polymers are also prone to morphological instability during storage at elevated T, often leading to macroscopic phase separation, and a thick layer of polymer at the blend surface [16, 26, 28, 29]. Metallocene catalyzed linear low density polyethylenes (m-LLDPE) have therefore recently been proposed as alternative modifiers for bitumen, because they combine low cost with improved dispersion characteristics and storage stability with respect to conventional polyolefins [30, 31]. Metallocene catalysis facilitates control of the molecular structure and molar mass distribution, providing polymers with relatively narrow molar mass distributions and a uniform distribution of short chain branches, for example [30, 32, 33]. This permits tuning of bulk properties such as viscosity and crystallinity and may lead to substantially reduced melt elasticity, which has been argued to account for the improved dispersions observed in the corresponding PMBs, since any differences in thermodynamic compatibility with bitumen between m-LLDPEs and other PE-based polymers may be assumed to be minor [30, 31]. This study focuses on the thermal and dynamic mechanical properties of PMBs prepared from two selected m-LLDPEs with contrasting melt flow indices, MFI, glass transition temperatures, T_g, melting temperatures, T_m, and degrees of crystallinity, in order to assess their potential for applications that currently make use of SBS-modified bitumens, and to provide pointers for future materials selection.

Experimental

A high penetration grade bitumen (180/220) was modified by blending with either an ethylene–butene (PE–B) or an ethylene–octene (PE–O) m-LLDPE copolymer (ENGAGE®

7447 and ENGAGE® 8402, respectively, supplied by Dow Chemical Company) at polymer concentrations ranging from 5 to 50 wt%. The properties of these copolymers are summarized in Table 1. In the blending procedure, which was chosen to simulate industrial processing conditions currently used for bitumen/SBS blends, stainless steel cans with a capacity of approximately 500 mL were filled with approximately 200–250 g of bitumen at 80 °C, and the required amount of polymer was gradually added. The cans were closed with a screw top perforated to accommodate a motorized four-blade stainless steel propeller. They were then immersed in an oil bath and T was raised to 180 °C. Each blend was mixed for 2.5 h at a stirring speed of 60 rpm after which it was removed from the can and left to cool to room T on silicone paper.

For the morphological investigations, the blends were heated and pressed between glass slides, and then observed by optical and fluorescence microscopy using an Olympus AX 70 optical microscope. The application of fluorescence microscopy to PMBs is based on the assumption that the polymer preferentially absorbs the fluorescent constituents of the base bitumen. The bitumen-rich phases thus appear dark in fluorescent light micrographs, while the phases containing the polymer appear light [8]. Image J (US National Institutes of Health) image analysis software was used to determine the projected volume fraction of the polymer-rich regions from the resulting images after suitable thresholding.

Thermal behavior was investigated by differential scanning calorimetry (DSC) using the Q100 from Thermal Analysis Instruments. Capsules containing between 5 and 10 mg of each specimen were subjected to repeated heating and cooling scans under nitrogen between −100 and 200 °C at a rate of 10 K/min. Since only minor differences were observed between the first and second heating scans, subsequent discussion will focus on the results from the first heating scans, which were considered to be more representative of the initial mixing conditions.

An ARES rheometer from thermal analysis instruments was used for dynamic shear tests. The plate–plate geometry was used to investigate the PMBs and pure polymers, with a plate diameter of 8–20 mm depending on the bitumen concentration and hence on the viscosity, and the Couette geometry was used for the unmodified bitumen. In each case, a strain sweep was carried out prior to the dynamic measurements and the dynamic strain amplitude was

chosen so as to remain within regimes in which the behavior was predominantly linear viscoelastic. $3 \times 1 \times 1$ cm^3 strips of the PMBs and pure polymers were also tested in dynamic tension using the Q800 dynamic mechanical analyzer from thermal analysis instruments. T was scanned from -50 to 50 °C at 1 Hz, typically at an applied strain of 0.1%, again in order to obtain a predominantly linear response.

Results and discussion

A two-phase morphology was observed in all the PMBs, as shown in the fluorescent light images in Fig. 1. PMBs containing 5 wt% PE–O (Fig. 1a) consisted of swollen polymer-rich inclusions with an average diameter of 20 μm dispersed in a continuous bitumen-rich phase. On the other hand, at 5 wt% PE–B (Fig. 1f), swelling of the polymer was already sufficient to result in phase inversion, the dispersed phase consisting of bitumen-rich inclusions with an approximately constant diameter of 4 μm. At higher polymer contents, all the PMBs showed a continuous polymer-rich phase and a dispersed bitumen-rich phase. The volume fractions of the polymer-rich phase estimated by image analysis are given in Fig. 2. As the polymer content increased, the volume fraction of the polymer-rich phase also increased and it remained significantly higher than the polymer weight fraction, indicating substantial swelling. Estimates of the corresponding volume fractions, ϕ_1, of bitumen in the polymer-rich phase are given in Fig. 3, obtained by assuming the densities of the different phases to be close to 1. The bitumen content of the polymer-rich phase decreased with increasing m-LLDPE content and was somewhat greater for PE–O than for PE–B. Moreover, the degrees of swelling at low m-LLDPE contents were comparable to those reported for SBS, i.e., a ninefold increase in volume for an overall m-LLDPE content of 5 wt%, which may be rationalized in terms of the literature values for the three-dimensional Hansen solubility parameters for bitumen [6, 7]; although polyethylenes do not show specific interactions with bitumen, the dispersive components of the solubility parameter, δ_D, for polyethylenes (about 17.5 MPa$^{1/2}$) and maltene (17.7 MPa$^{1/2}$) are relatively close, implying considerable overlap between their respective solubility spheres [6]. Moreover, asphaltene, as defined by SARA fractionation, is inferred to be far less soluble in polyethylene owing to its stronger dispersive interactions ($\delta_D = 19.6$ MPa$^{1/2}$) rather than differences in polarity. Therefore, the heterogeneous microstructures observed in the present case may be considered to result from precipitation of asphaltene-rich domains from a continuous phase composed essentially of

maltene and m-LLDPE regardless of whether the asphaltene forms a separate phase in the original bitumen.

Differential scanning calorimetry traces are shown in Figs. 4 and 5 for PE–O and PE–B and the corresponding PMBs. The DSC trace for pure bitumen showed a broad low T transition comprising two distinct steps in heat capacity, the more marked of these at -50 °C generally being attributed components of the maltene fraction [5, 34]. Melting peaks were apparent in both polymer modifiers, but the relatively sharp peak observed for pure PE–O at around 96 °C suggested a narrower distribution of lamellar thicknesses than for PE–B, which showed a broad peak with a maximum at about 35 °C. The enthalpies of fusion, ΔH_f, of the as-received resins were estimated from the DSC traces to be 113 and 37 J/g for PE–O and PE–B, respectively, which correspond to degrees of crystallinity of 40 and 13% by weight, if the enthalpy of fusion of 100% crystalline polyethylene homopolymer is taken to be 283 J/g [14]. The glass transition in both types of m-LLDPE ($T_g = -36$ and -53 °C in PE–O and PE–B, respectively) overlapped with the range of T corresponding to the glass transition in the bitumen. As shown in Figs. 4 and 5, addition of the m-LLDPE resulted in a single glass transition, and T_g tended toward that of the pure polymer as the polymer content was increased (Fig. 6).

The T_m of the polymer-rich phase, defined as the value of T corresponding to the maximum in the melting endotherm, were reduced by up to 20 K with respect to those of the pure polymers, as shown in Fig. 7. The largest decreases in T_m occurred at the lowest polymer concentrations, i.e., at relatively high concentrations of bitumen in the polymer-rich phase (cf. Fig. 3), consistent with previous studies of blends of bitumen with semicrystalline polymers [14, 17, 18, 22]. Such behavior might in principle be accounted for in terms of expressions for the depression of T_m of a semicrystalline polymer in the presence of a low molar mass solvent derived from the Flory–Huggins theory for the thermodynamics of polymer–solvent mixtures. For low ϕ_1, this leads to:

$$\frac{1}{T_m} - \frac{1}{T_m^0} = \frac{RV_{pu}}{V_1 \Delta H_{pu}}(\phi_1 - \chi\phi_1^2) \qquad (1)$$

where T_m^0 is the melting point of the pure polymer, V_{pu} is the molar segmental volume of the polymer, V_1 is the molar volume of the solvent, ΔH_{pu} is the molar enthalpy of crystallization per segment of the pure polymer (taken to be 4100 J/CH$_2$ [14]), and χ is the Flory–Huggins interaction parameter [35]. In the present case of a heterogeneous solvent, whose composition is also expected to vary with its concentration in the polymer, V_1 and χ are poorly defined. However, assuming χ to be of the order of 0.5, Eq. 1 provides a reasonable fit to the variation in T_m with ϕ_1 for both polymers at low ϕ_1 implied by Fig. 7 for

Fig. 1 Fluorescence micrographs of m-LLDPE modified bitumen: PE–O: **a** 5 wt%, **b** 10 wt%, **c** 20 wt%, **d** 30 wt%, **e** 50 wt%; PE–B: **f** 5 wt%, **g** 10 wt%, **h** 20 wt%, **i** 30 wt%, **j** 50 wt%
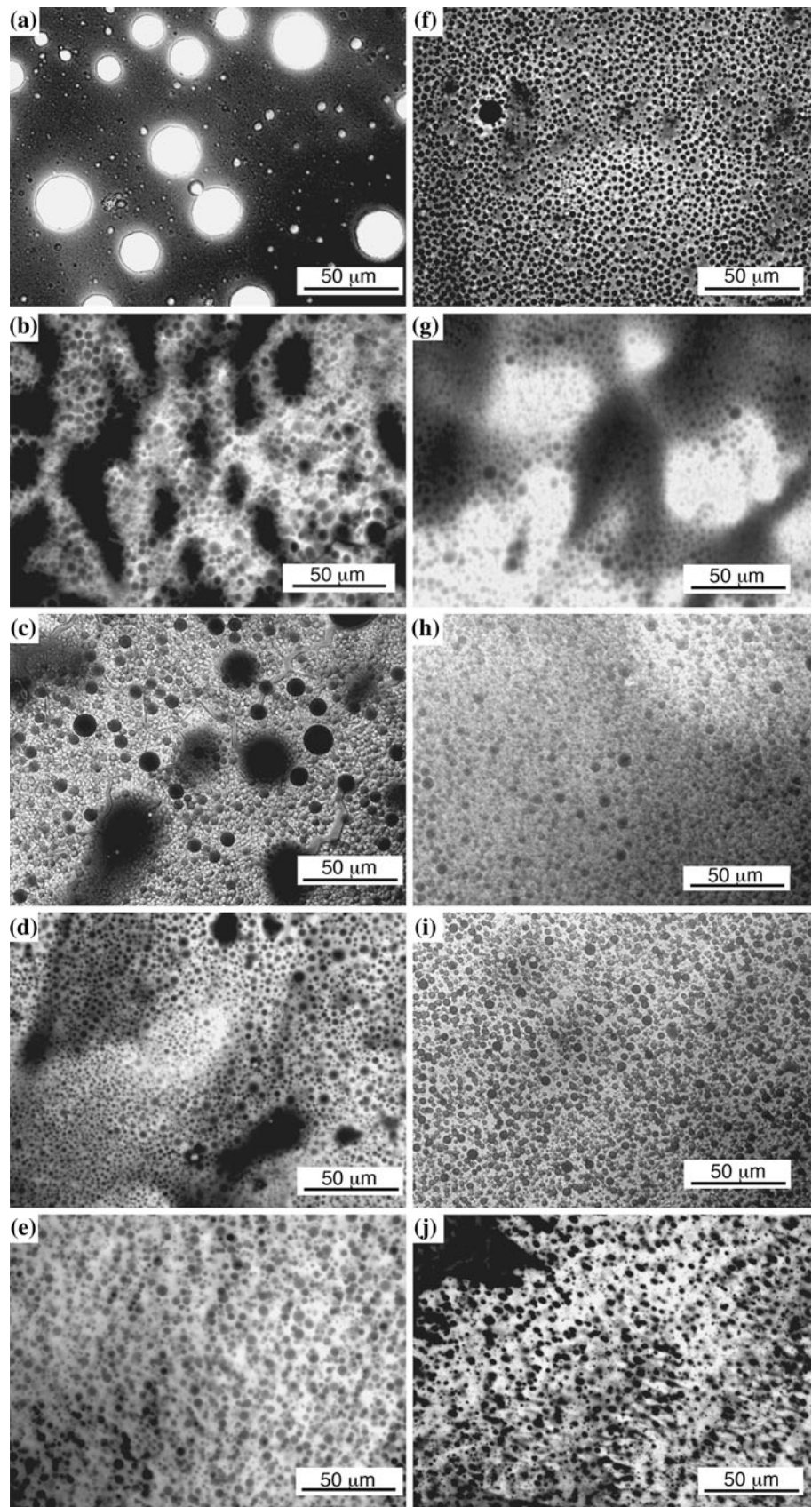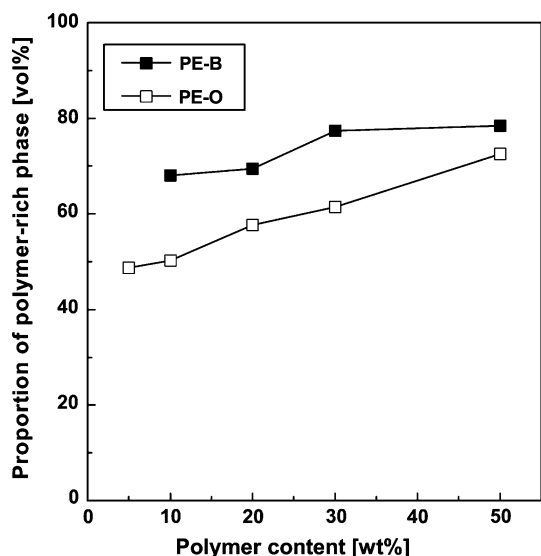
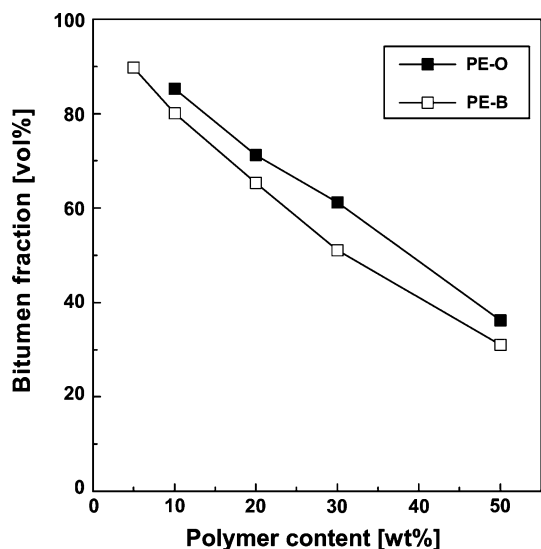**Fig. 2** Volume fraction of the polymer-rich phase in the PMBs as a function of the polymer content

Fig. 3 Bitumen content in the polymer-rich phase as a function of the overall polymer content of the PMBs

$V_{pu}/V_1 = 0.2$. Bearing in mind the limitations of the Flory–Huggins approach in the present context, this suggests similar affinities between the two different m-LLDPE and the bitumen. Hence, the greater solubility of the maltene in PE–O inferred, e.g., from Fig. 3, may be a consequence of the higher MFI of this latter (which implies a lower average molar mass).

The variation of ΔH_f with composition estimated from the DSC traces for the PMBs is shown in Fig. 8. In each case, ΔH_f increased roughly monotonically with increasing polymer content (absolute values were difficult to determine with precision owing to uncertainties in the baseline, particularly in the case of the PE–B-based PMBs, in which
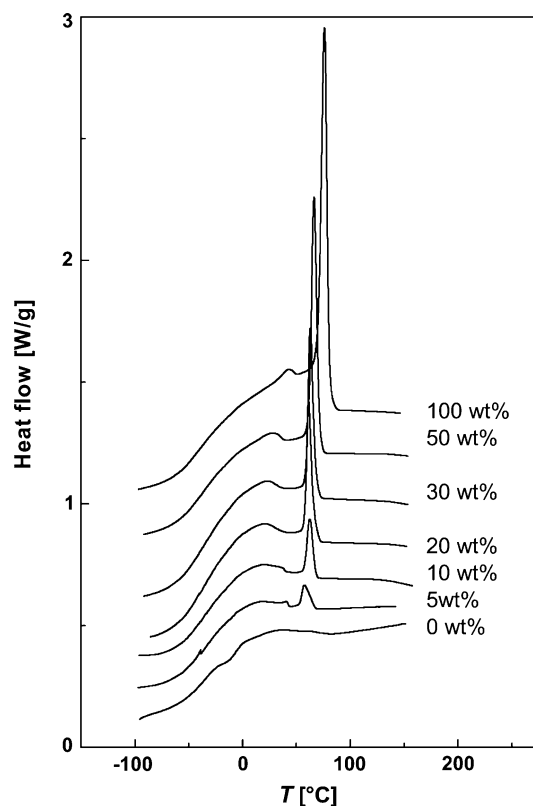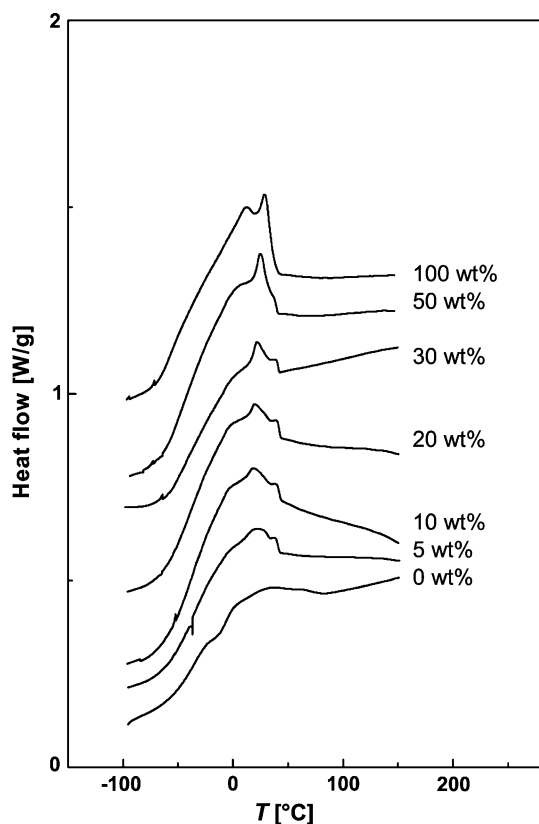

Fig. 4 DSC heating scans for pure bitumen and PE–O modified bitumen

the melting transition overlapped with the glass transition; in future study, it would therefore be of interest to use modulated DSC, which allows one to separate reversing and non-reversing components of the heat flow signal and hence deconvolute melting peaks and glass transitions under appropriate scanning conditions). However, the increases in ΔH_f with polymer content appeared greater at low polymer contents than would be expected on the basis of simple proportionality with the polymer content, indicating increased crystallinity in the presence of the bitumen and/or co-crystallization of part of the bitumen. Similar trends were observed by Fawcett et al. [17], who found that PMBs containing LLDPE with a relatively high degree of crystallinity showed further increases in the apparent degree of crystallinity of the LLDPE with decreasing polymer content, although they reported the opposite behavior for a less crystalline LDPE.

Tensile storage moduli (E') and loss angle ($\tan \delta$) of the PMBs and pure polymers are shown in Figs. 9 and 10. The tests were carried out at T up to 50 °C, beyond which, all the materials became too soft to allow precise determination of the tensile stress in the linear viscoelastic regime. Even under these conditions, satisfactory measurements were only possible for PMBs with relatively high polymer contents. As shown in Fig. 9, E' for the pure PE–B
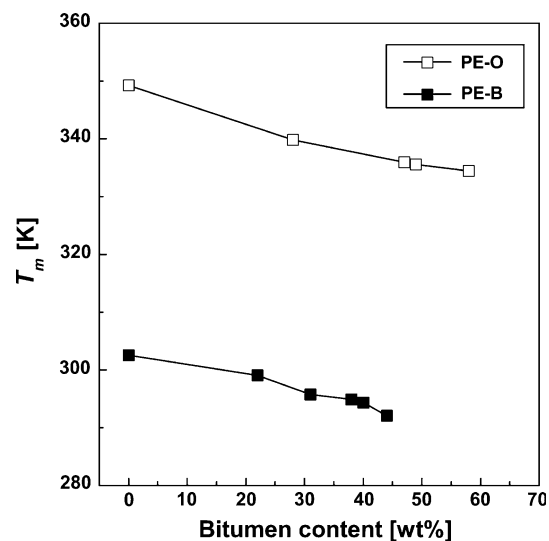
Fig. 5 DSC heating scans for pure bitumen and PE–B modified bitumen
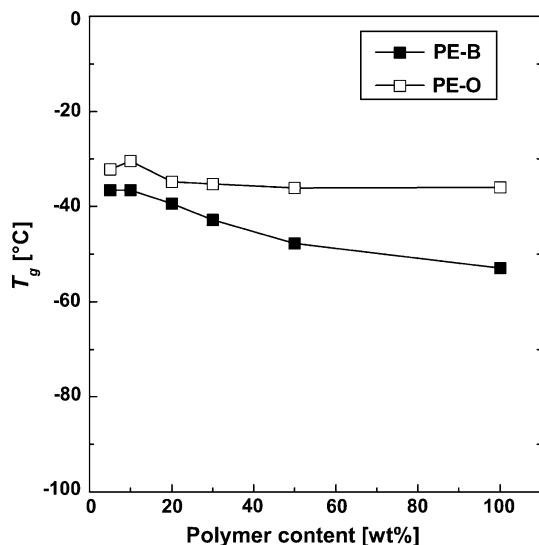
Fig. 6 Glass transition temperature, T_g, as a function of polymer content for the different PMBs

Fig. 7 Melting temperature, T_m, as a function of bitumen content in the polymer-rich phase for the different PMBs

Fig. 8 Heat of fusion, ΔH_f, for the different PMBs

decreased by about two orders of magnitude over the range of T investigated, and a rubbery plateau was present between approximately −20 and 30 °C, melting leading to a sharp drop in E' at higher T. At very low T, there was also a suggestion of a second plateau corresponding to the
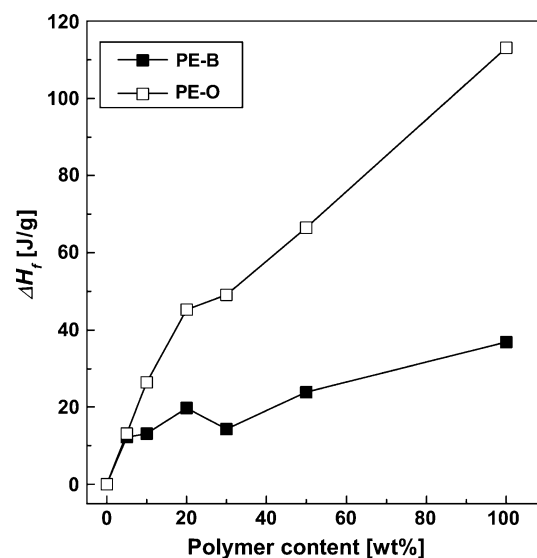
glassy regime below T_g. As the bitumen content increased in the PMBs containing PE–B, the rubbery plateau became restricted to T immediately below T_m. Moreover, E' showed a monotonic increase with bitumen content at low T, so that at −50 °C, E' for the PMB containing 20 wt% polymer was about one order of magnitude greater than that of the pure polymer, consistent with the higher low T stiffness of the bitumen in this case. However, the curves for the different materials converged as T increased. As also shown in Fig. 9, there was a broad peak in tan δ centered at about −50 °C in the pure PE–B, corresponding to the γ-transition, which is generally associated with the glass transition, consistent with the DSC results [36]. This low T peak shifted to higher T as the bitumen content
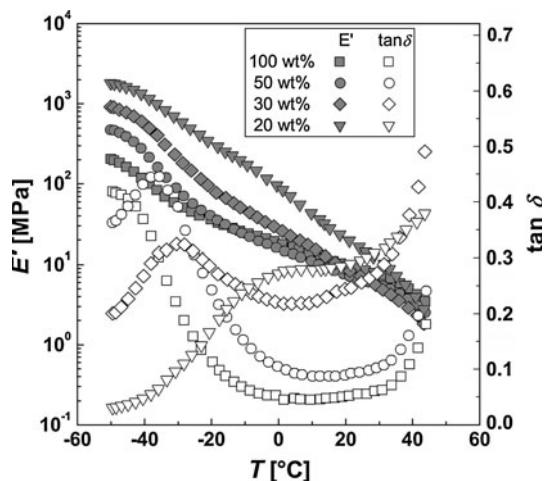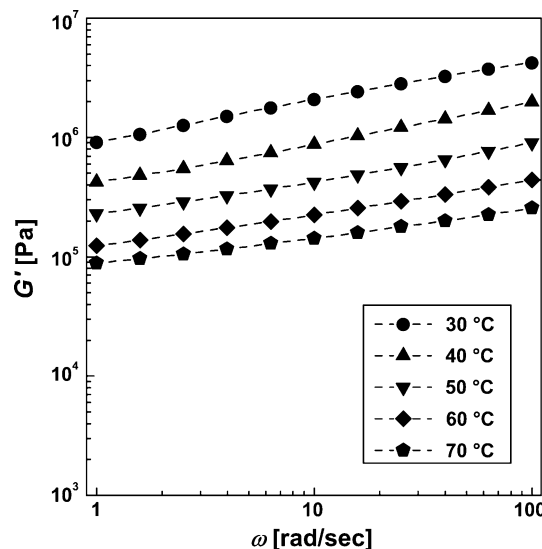
Fig. 9 Variation in tensile storage modulus E' and in the loss angle, tan δ, with composition for PE–B and PMBs containing PE–B
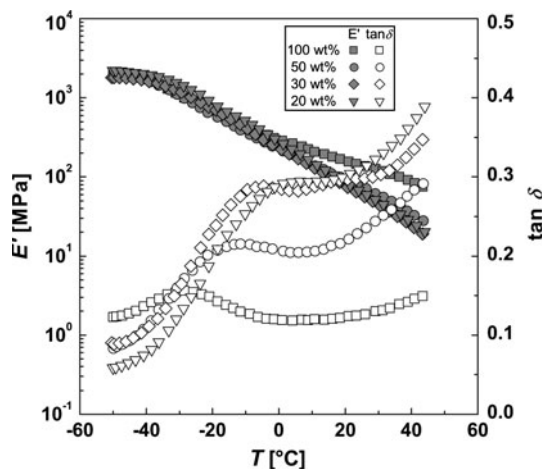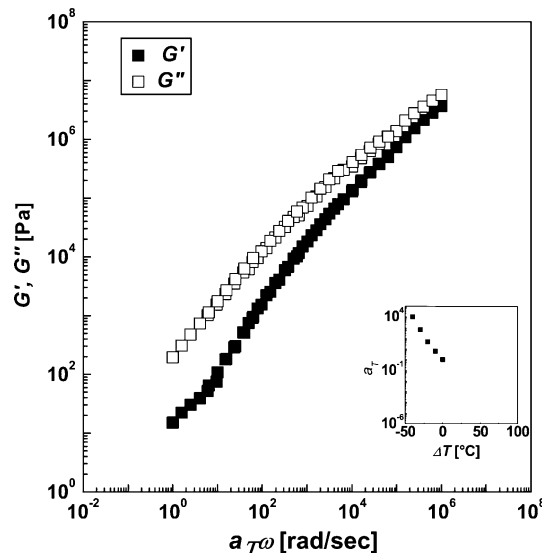

Fig. 10 Variation in tensile storage modulus E' and in the loss angle, tan δ, with composition for PE–O and PMBs containing PE–O
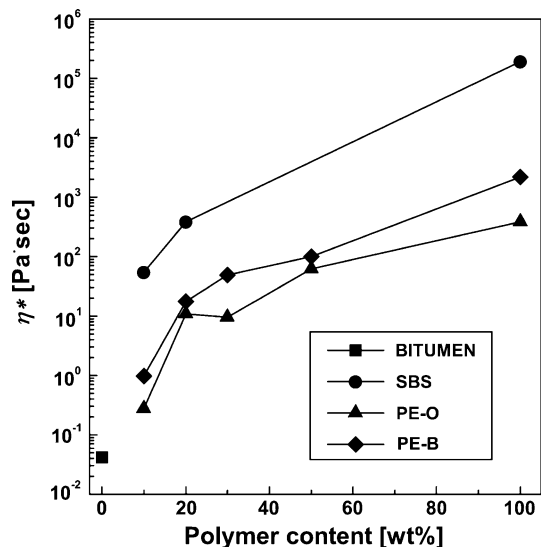
Fig. 11 Complex viscosity, η^*, as measured at 180 °C for pure bitumen and different PMBs

Fig. 12 Shear storage modulus, G', of 20 wt% PE–O PMB at different T

Fig. 13 Master curves of the dynamic viscoelastic functions of the unmodified bitumen at a reference temperature $T_r = 50$ °C. The *inset* shows the corresponding shift factors, a_T, as a function of $\Delta T = T - T_r$

increased. Data for E' and tan δ are given in Fig. 10 for PE–O and the corresponding PMBs. The curves for E' were very close for all the PMBs based on PE–O at low T, reflecting the relatively high degree of crystallinity, high T_g and hence high stiffness of the PE–O at low T. Indeed, increasing the bitumen content led to a decrease in E' at high T. As with PE–B, PE–O showed a broad peak in tan δ corresponding to the γ-transition, which again shifted to slightly higher T as the bitumen content increased.

Fig. 14 Master curves of the dynamic viscoelastic functions of PMBs containing PE–B at a reference temperature $T_r = 50$ °C. The *inset* shows the corresponding shift factors, a_T, as a function of $\Delta T = T - T_r$
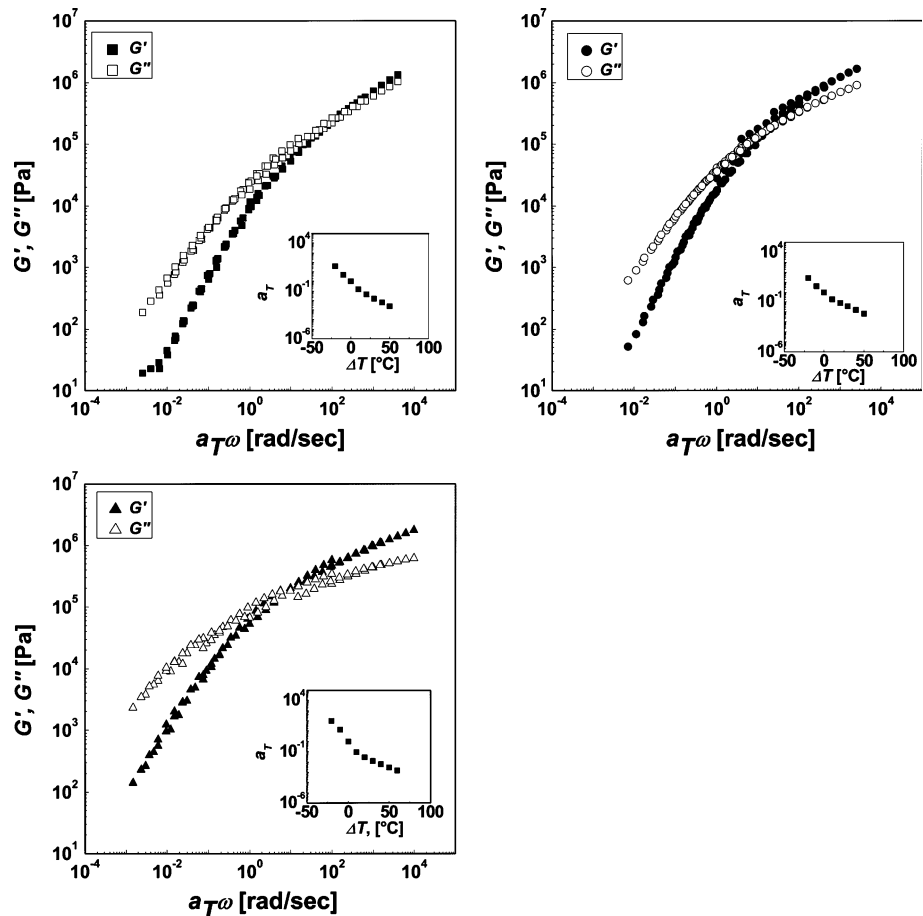

Figure 11 shows the magnitude of the complex viscosity, η^*, of the PMBs and pure polymers at the mixing temperature of 180 °C and a frequency of 1 Hz, along with results from blends modified with SBS copolymer for comparison. Regardless of the type of polymer additive, the PMBs showed significantly higher viscosity than the unmodified bitumen. However, the viscosity increases were far greater for the specific grade of SBS investigated here (C-311 from Repsol®) than for both types of m-LLDPE, reflecting the high viscosity of the pure SBS, so that the viscosity of a PMB containing 10 wt% SBS was comparable with a PMB containing 50 wt% PE–B. Indeed, the viscosity of the pure PE–O was less than an order of magnitude greater than the PMB containing 10 wt% SBS.

Figure 12 shows a representative example of the evolution of the dynamic shear storage modulus, G', in the PMBs as a function of frequency at different T (in this case for a PMB containing 20 wt% PE–O). G' increased monotonically with both frequency and T in all the materials, and, as suggested by Fig. 12, the data could generally be superposed by lateral shifts along the T axis. Time–temperature superposition was therefore used to provide an indication of the response at a reference temperature of 50 °C (representative of the upper range of service

temperatures) over an extended frequency range, as shown in Figs. 13, 14, 15, where master curves for G' and the loss modulus, G'', are given as a function of frequency for pure bitumen and the PMBs containing up to 30 wt% m-LLDPE, along with the corresponding shift factors, $a_T(T)$. The data showed reasonable overlap in this composition range, but it should be emphasized that bitumen is known to be a thermo-rheologically complex material, as discussed extensively elsewhere, so that the absolute frequency scale should be treated with caution [24, 37, 38]. On the other hand, the $a_T(T)$ were similar for the different PMBs, so that the master curves provided a convenient means of comparing their overall behavior.

The unmodified bitumen showed a predominantly viscous response (Fig. 13), the loss modulus G'' exceeding the storage modulus G' at all the frequencies and T investigated, although the curves tended to converge at the highest frequencies/lowest T, consistent with previous observations [30]. The PMBs containing PE–B also showed a viscous response at low frequencies (Fig. 14), with G' and G'' proportional to ω^{-1} and ω^{-2}, respectively in the limit $\omega \to 0$, consistent with the expected behavior for a linear polymer melt in the terminal zone. However, as the frequency increased and/or T decreased there was a

Fig. 15 Master curves of the dynamic viscoelastic functions of PMBs containing PE–O at a reference temperature $T_r = 50\ ^\circ\text{C}$. The *inset* shows the corresponding shift factors, a_T, as a function of $\Delta T = T - T_r$
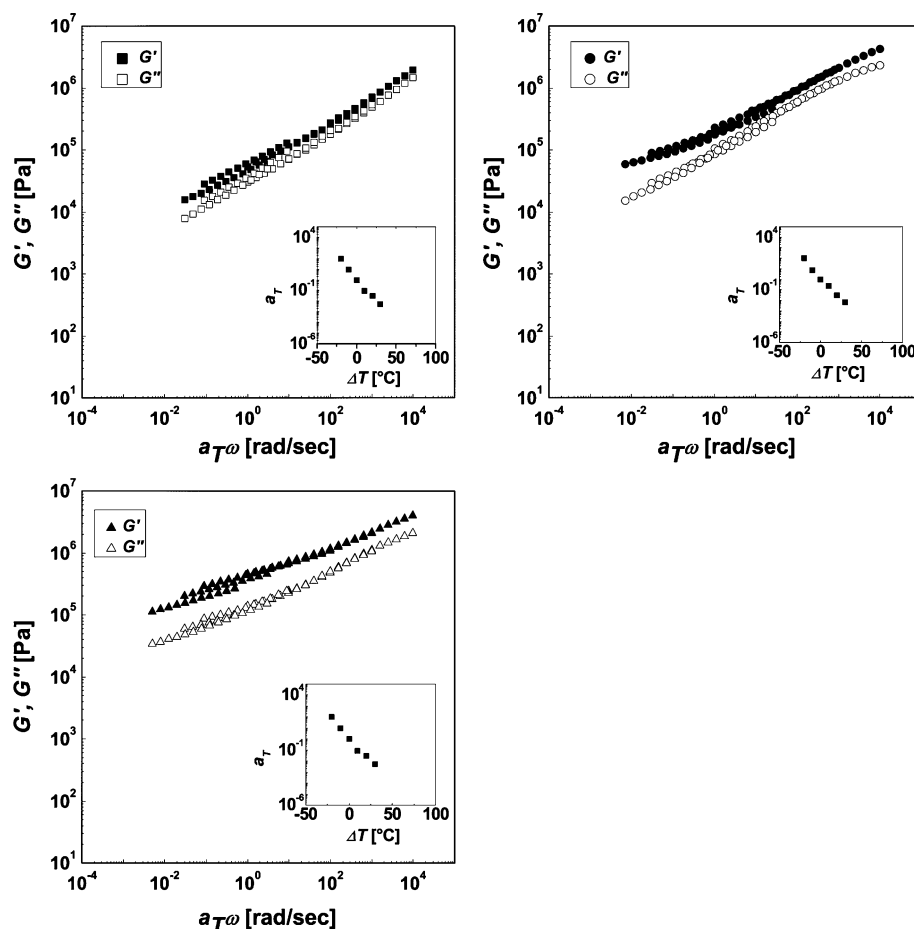
crossover between G' and G'', which became more apparent at higher polymer contents, reflecting an increasingly elastic response. The apparent crossover frequency, ω_c, at the reference temperature of 50 °C used for the superposition, and the corresponding values of G' and G', did not change markedly with PE–B content, although ω_c did increase somewhat as the PE–B content was reduced from 20 to 10 wt%. A similar crossover has been reported in other polyolefin-based PMBs, along with an increase in ω_c for the PMBs with respect to that observed in the pure polymer, which has been attributed to the plasticizing effect of the bitumen [30]. In the case of the PE–O-based PMBs (Fig. 15), G' remained greater than G'' over the entire frequency range, even at the lowest PE–O contents, indicating predominantly elastic behavior, although the differences in G' and G'' increased as the polymer content increased. Moreover, the frequency dependence of G' was also relatively weak in these materials, implying improved long-term mechanical stability at T in the vicinity of 50 °C.

These initial results for m-LLDPE-based PMBs are promising in that they indicate similar compatibility with the bitumen to that observed for SBS, in spite of the significant differences in polarity between SBS and m-LLDPE, which is important for the morphological

stability, and they also confirm that relatively good dispersions may be obtained under standard processing conditions. Significant improvements in low T flexibility have been observed, the PMBs containing PE–B, in particular, showing significantly reduced stiffness down to T in the range of −50 °C, whereas PMBs containing SBS tend to harden below −30 °C [39]. Moreover, dynamic viscosity measurements showed that it should be possible to envisage a relatively wide range of compositions without substantial modification to mixing and processing procedures currently used for SBS, which has the disadvantage of being more expensive and more sensitive to UV exposure.

High T stability, nevertheless, remains a concern with the m-LLDPEs considered in this study, owing to the relatively low T_m of the m-LLDPE-rich phase, the onset of melting being evident from the substantial decreases in E' from T as low as 40 °C in the PE–B-based PMBs (Fig. 9), which is incompatible with industrial criteria for outdoor applications (PMBs containing SBS show a rubbery plateau that extends up to about 80 °C). The melting onset in pure PE–O occurred at significantly higher T (cf. Table 1), but there remained a significant loss in stiffness for $T > 40$ °C in the PE–O-based PMBs. These latter continued to show essentially elastic behavior in this range of T,

implying improved high T stability, albeit at the expense of increased crystallinity and low T stiffness, but it is clear that even in this case, the high T response must be improved if practical implementation is to be envisaged. It may nevertheless be possible to exploit the relatively good miscibility of m-LLDPEs with other polyolefins (other LLPDEs or LDPE) in order to tailor the high T response of the polymer modifier and hence the melting behavior of the PMB, and the results also imply considerable scope for controlling the low T response by varying the degree of crystallinity and T_g. This will provide the focus for the next stage of the study, in which a compromise will be sought between high T stability and low T elasticity, in order to provide a material that corresponds to current industrial norms.

Conclusions

The two types of m-LLDPE investigated in this study as additives for PMBs show some promising characteristics, notably reduced low T stiffness with respect to PMBs modified with SBS and relatively low viscosities up to high polymer contents in the range of T corresponding to typical PMB processing temperatures. Fluorescence microscopy showed a continuous polymer-rich phase to be present in the m-LLDPEs over most of the composition range investigated, indicating a high degree of solubility of the bitumen in the respective polymers. However, the presence of the bitumen led to a significant reduction in T_m in the polymer-rich phase, and hence excessive softening of the PMBs based on a relatively low T_m m-LLDPE for T exceeding 40 to 50 °C. Blending with a higher T_m m-LLDPE led to better high temperature stability, but, in the present case, this was accompanied by a higher degree of crystallinity and a higher T_g, which may limit improvements in low T flexibility. These results therefore suggest that the overall properties may need to be tailored by blending different m-LLDPE and/or other compatible polyolefins in order to achieve an optimum compromise between high and low T performance.

References

1. Airey GD (2004) J Mater Sci 39:951. doi:10.1023/B:JMSC.0000012927.00747.83
2. Isacsson U, Lu X (1995) Mater Struct 28:139
3. Read J, Whiteoak D (2003) The Shell bitumen handbook, 5th edn. Thomas Telford, London
4. Loeber L, Muller G, Morel J, Sutton O (1998) Fuel 77:1443
5. Lesueur D (2009) Adv Colloid Interface Sci 145:42
6. Redelius PG (2004) Energy Fuels 18:1087
7. Hansen CM (2007) Hansen solubility parameters: a user's handbook, 2nd edn. CRC Press, Boca Raton
8. Ait-Kadi A, Brahimi B, Bousmina M (1996) Polym Eng Sci 36:1724
9. Lu X, Isacsson U (2001) Polym Test 20:77
10. Airey GD (2002) Construct Build Mater 16(8):473
11. Yildirim Y (2007) Construct Build Mater 21:66
12. Fawcett AH, Lor SK (1992) Polymer 33(9):2003
13. Oba K, Bjork F (1993) Polym Test 12:35
14. Fawcett AH, McNally T, McNally GM, Andrews F, Clarke J (1999) Polymer 40:6337
15. Oba K, Roller A (1995) Mater Struct 28:596
16. Giavarini C, De Filippis P, Santarelli ML, Scarsella M (1996) Fuel 75:681
17. Fawcett AH, McNally T, McNally GM (1999) J Elastom Plast 31:334
18. Isacsson U, Lu X (1999) J Mater Sci 34:3737. doi:10.1023/A:1004636329521
19. Lu X, Isacsson U, Ekblad J (1999) Mater Struct 32:131
20. Fawcett AH, McNally T (2000) Polymer 41:5315
21. Fawcett AH, McNally T (2001) Polym Eng Sci 41:1251
22. Fawcett AH, McNally T, McNally G (2002) Adv Polym Technol 21:275
23. Yousefi AA (2002) J Appl Polym Sci 90:3183
24. Gonzalez O, Munoz ME, Santamaria A, Garcia-Morales M, Navarro FJ, Partal P (2004) Eur Polym J 40:2365
25. Perez-Lepe A, Martinez-Boza FJ, Gallegos C (2005) Energy Fuels 19:1148
26. Polacco G, Muscente A, Biondi D, Santini S (2006) Eur Polym J 42:1113
27. Sengoz B, Isikyakar G (2008) Construct Build Mater 22:1897
28. Hesp SAM, Woodhams RT (1991) Colloid Polym Sci 269(8):825
29. Perez-Lepe A, Martinez-Boza FJ, Gallegos C (2007) J Appl Polym Sci 103:1166
30. Rojo E, Fernandez M, Pena JJ, Pena B, Munoz ME, Santamaria A (2004) Polym Eng Sci 44(9):1792
31. Gonzalez O, Munoz ME, Santamaria A (2006) Rheol Acta 45:603
32. Hamielec AE, Soares JBP (1996) Prog Polym Sci 21:651
33. Liu C, Wang J, He J (2002) Polymer 43:3811
34. Masson J-F, Polomark G, Collins P (2005) Thermochim Acta 436:96
35. Mandelkern L, Garrett RR, Flory PJ (1952) J Am Chem Soc 74:3949
36. Lee H, Cho K, Ahn TK, Choe S, Kim IJ, Park I, Lee BH (1997) J Polym Sci B 35:1633
37. Lesueur D, Gérard JF, Claudy P, Létoffé JM, Martin D, Planche JP (1998) J Rheol 42:1059
38. Lesueur D, Gérard JF, Claudy P, Létoffé JM, Martin D, Planche JP (1996) J Rheol 40:813
39. Becker YM, Muller AJ, Rodriguez Y (2003) J Appl Polym Sci 90:1772